Russian Journal of General Chemistry, Vol. 73, No. 5, 2003, pp. 675–683. Translated from Zhurnal Obshchei Khimii, Vol. 73, No. 5, 2003, pp. 715–723.
Original Russian Text Copyright © 2003 by Oparin, Fedotova, Trostin.

Structural Parameters of Concentrated Aqueous Solutions of Lithium Chloride under Extreme Conditions, Determined by the Method of Integral Equations: Effect of Isothermal Compression

R. D. Oparin, M. V. Fedotova, and V. N. Trostin

Institute of Solution Chemistry, Russian Academy of Sciences, Ivanovo, Russia

Received February 28, 2001

Abstract—The structure formation in aqueous solutions of LiCl, LiCl : nH$_2$O (n = 3.15, 8.05, 14.90), under conditions of isothermal compression (T 523 K, P 100–1500 bar) was studied by the method of integral equations. Isothermal compression only weakly affects the structure of the bulk solvent. Irrespective of the solution concentration, tetrahedral ordering of water molecules is absent in the entire pressure range, and the number of O–H bonds does not change noticeably. In all the solutions, compression slightly enhances the coordinative power of both ions. The content of hydration-separated ion pairs somewhat grows, and the content of contact ion pairs slightly decreases.

Proceeding with studies on structural properties of aqueous electrolyte systems under extreme conditions [1–4], we examined the effect of isothermal compression on the structure formation in concentrated aqueous solutions of lithium chloride. Virtually no studies were made on this subject previously, and available data mostly concern the effect of temperature at standard or moderately high temperatures (see, e.g., [5–10]). This is due to experimental difficulties associated with high parameters of state and to relatively long time required for computer simulation.

In this work, the structural characteristics of aqueous LiCl solutions under conditions of isothermal compression were evaluated by the method of integral equations in which the structural and thermodynamic characteristics of objects are calculated from the known potentials of interparticle interactions. In contrast to computer simulation, the method of integral equations, similarly to direct structural methods, gives a diffusion-averaged structural pattern of liquid-phase systems and requires much shorter computation time. Structural data obtained by the method of integral equations are reasonably consistent with the available experimental structural data and results of computer simulation for standard parameters of state.

As a model of aqueous electrolyte solutions we chose a mixture of water molecules and ions with the water–water, ion–water, and ion–ion pair potentials of the following kinds. For water, we used the SPC model [11]; the parameters of its modified version are given in [12]. The short-range interactions between ions and water molecules were described by the Lennard–Jones potential, and the long-range interactions, by the Coulombic potential. The ion–ion interactions were described by the Huggins–Meyer potential. The parameters of ion–water and ion–ion pair potentials are given in [13].

The structural characteristics of aqueous LiCl solutions were calculated by the Ornstein–Zernicke atom–atom integral equation [14], which has the following form in the case of ion–molecule systems:

$$\left.\begin{aligned}\rho_W \hat{h}_{WW}(k) &= \hat{s}_{WW}(k)\hat{c}_{WW}(k)\hat{s}_{WW}(k)\\ &\quad + \rho_W \hat{s}_{WW}(k)\hat{c}_{WW}(k)\hat{h}_{WW}(k),\\ \hat{h}_{IW}(k) &= \hat{c}_{IW}(k)\hat{s}_{WW}(k) + \rho_W \hat{c}_{IW}(k)\hat{h}_{WW}(k)\\ \hat{h}_{II}(k) &= \hat{c}_{II}(k) + \rho_W \hat{c}_{IW}(k)\hat{h}_{IW}(k)\\ &\quad + \rho_I \hat{c}_{II}(k)\hat{h}_{II}(k)\end{aligned}\right\} \qquad (1)$$

Here, ρ_W is the density of solvent molecules; ρ_I, density of ions; $\hat{h}_{\alpha\beta}(k)$, $\hat{c}_{\alpha\beta}(k)$, and $\hat{s}_{\alpha\beta}(k)$, matrices consisting of the following elements:

$$\hat{h}^{xy}_{\alpha\beta}(k) = \frac{4\pi}{k}(\rho_x\rho_y)^{1/2}\int_0^\infty r dr h^{xy}_{\alpha\beta}(r)\sin(kr),$$

$$\hat{c}^{xy}_{\alpha\beta}(k) = \frac{4\pi}{k}(\rho_x\rho_y)^{1/2}\int_0^\infty r dr c^{xy}_{\alpha\beta}(r)\sin(kr),$$

$$\hat{s}^{xy}_{\alpha\beta}(k) = \delta_{xy}\left[\delta_{\alpha\beta} + (1-\delta_{\alpha\beta})\frac{\sin(kl^x_{\alpha\beta})}{kl^x_{\alpha\beta}}\right].$$

1070-3632/03/7305-0675 $25.00 © 2003 MAIK "Nauka/Interperiodica"

Here, ρ_x is the density of molecules of kind x; ρ_y, density of molecules of kind y; $l^x_{\alpha\beta}$, intramolecular distance between force centers α and β belonging to a molecule of kind x; $h^{xy}_{\alpha\beta}(r)$ and $c^{xy}_{\alpha\beta}(r)$, overall and direct atom–atom correlation functions of force centers α and β belonging to molecules of kinds x and y; $\hat{s}^{xy}_{\alpha\beta}(r)$, Fourier transformant matrix of the function describing intramolecular correlations; δ_{xy}, Dirac delta function; and $\delta_{\alpha\beta}$, Kronecker delta symbol.

For system of Eqs. (1), we used hyperchain closure (2).

$$\left.\begin{aligned} h_{\mathrm{WW}}(r) + 1 \equiv g_{\mathrm{WW}}(r) &= \exp[-BU_{\mathrm{WW}}(r) \\ &\quad + h_{\mathrm{WW}}(r) - c_{\mathrm{WW}}(r)], \\ h_{\mathrm{IW}}(r) + 1 \equiv g_{\mathrm{IW}}(r) &= \exp[-BU_{\mathrm{IW}}(r) \\ &\quad + h_{\mathrm{IW}}(r) - c_{\mathrm{IW}}(r)], \\ h_{\mathrm{II}}(r) + 1 \equiv g_{\mathrm{II}}(r) &= \exp[-BU_{\mathrm{II}}(r) \\ &\quad + h_{\mathrm{II}}(r) - c_{\mathrm{II}}(r)]. \end{aligned}\right\} \qquad (2)$$

Here, $g(r) \equiv g^{xy}_{\alpha\beta}(r)$ is the pair atom–atom correlation function of force centers α and β belonging to molecules of kinds x and y; $-BU(r) \equiv -BU^{xy}_{\alpha\beta}(r) = -B[\eta^{xy}_{\alpha\beta}(r) + \Phi^{xy}_{\alpha\beta}(r)]$, initial atom–atom interaction potential (as a sum of short- and long-range components); $B = (k_{\mathrm{B}}T)^{-1}$, where k_{B} is the Boltzmann constant.

Solution of the Ornstein–Zernicke atom–atom equation for a system with the long-range electrostatic interaction requires renormalization of the initial long-range potential so that the equation include only the renormalized long-range interaction, shielded potential. This procedure, and also a procedure for numerical solution of the Ornstein–Zernicke atom–atom equation in the hyperchain approximation, are described in detail in [15].

By calculations in terms of the method of integral equations, we obtained for aqueous LiCl solutions, LiCl : nH$_2$O (n = 3.15, 8.05, 14.90), the pair correlation functions $g_{\alpha\beta}$ for T 523 K and P 100, 200, 500, 1000, and 1500 bar. From these data, we determined the interparticle distances and made conclusions on the presence and kind of ionic associates in solutions. Also, we calculated the coordination numbers of particles:

$$n_{\alpha\beta}(r) = 4\pi\rho\beta \int_0^r d_{\alpha\beta}(r) r^2 dr,$$

where ρ_β is the density of particles of kind β (Å^{-3}) coordinated with a particle of kind α. From the relative changes in the coordination numbers of particles [$\Delta n_{\alpha\beta}(r_{m1})$], we evaluated how the structural parameters of the solvent and the associative and coordinative powers of ions vary depending on the external parameters of state.

$$\Delta n_{\alpha\beta}(r_{m1}) = \frac{n^{P}_{\alpha\beta}(r_{m1}) - n^{100}_{\alpha\beta}(r_{m1})}{n^{100}_{\alpha\beta}(r_{m1})} \times 100\%.$$

Here, $n^{P}_{\alpha\beta}(r_{m1})$ is the coordination number of a particle at a pressure of 200, 500, 1000, and 1500 bar; r_{m1}, position of the first minimum of the pair correlation function $g_{\alpha\beta}(r)$.

The accuracy of direct and Newton–Raphson iterations in solution of the Ornstein–Zernicke atom–atom integral equation was 10^{-3}, and the accuracy of the evaluated coordination numbers of particles, 10^{-2}.

The structural parameters of the systems in hand are given in Tables 1–3. As seen from these data, the pressure exerts the strongest effect on the structure of the LiCl : 14.90H$_2$O solution (Table 1). As the characteristic values of the pair correlation functions for this solution under conditions of isothermal compression are close, the functions in Figs. 1–4 are shown only for the lowest (100 bar) and the highest (1500 bar) pressures.

WATER–WATER (W–W) CORRELATIONS

O–O. Our preliminary studies [16] showed that, in solutions of similar concentrations at 523 K and 100 bar, there is no continuous tetrahedral network of hydrogen bonds in the solvent [no corresponding peak in the $g_{\mathrm{O-O}}(r)$ function]. This fact is also confirmed by the results of theoretical and experimental structural studies for pure water (see, e.g., [17, 18]). As the pair correlation function $g_{\mathrm{O-O}}(r)$ at 523 K has no first minimum, it is impossible to distinguish the interaction between the water molecules that are the nearest neighbors from the interactions between the water molecules located in the points of the tetrahedral network. Therefore, in what follows, we will use as a structural characteristic the quantity $n^{(\mathrm{I+II})}_{\mathrm{O-O}}(r_{m2})$. This quantity is calculated for the distance corresponding to the second minimum of the pair function $g_{\mathrm{O-O}}(r)$ and is the sum of the quantities $n^{(\mathrm{I})}_{\mathrm{O-O}}(r_{m1})$ and $n^{(\mathrm{II})}_{\mathrm{O-O}}(r_{m2})$ (numbers of water molecules that are the nearest neighbors and the tetrahedrally ordered water molecules, respectively).

As the pressure is increased, the main peak in the $g_{\mathrm{O-O}}(r)$ function for the LiCl : 14.90H$_2$O solution slightly grows in intensity, and its maximum very slightly shifts toward shorter distances (Fig. 1, Table 1). The plateau in the range 0.430 – 0.450 nm

Table 1. Characteristic values of some pair correlation functions $g_{\alpha\beta}(r)$ and functions $n_{\alpha\beta}(r)$ for the LiCl : 14.90H_2O system under conditions of isothermal compression (T 523 K, P 100–1500 bar)

Parameter[a]	100 bar	200 bar	500 bar	1000 bar	1500 bar
$g_{\mathrm{O-O}}(r_{M1})$	2.306 (0.292)	2.314 (0.292)	2.339 (0.290)	2.374 (0.290)	2.406 (0.290)
$g_{\mathrm{O-O}}(r_{m2})$	0.899 (0.468)	0.897 (0.466)	0.894 (0.464)	0.888 (0.460)	0.882 (0.456)
$n_{\mathrm{O-O}}^{(\mathrm{I+II})}(r_{m2})$	10.75 (0.468)	10.75 (0.466)	10.75 (0.464)	10.74 (0.460)	10.73 (0.456)
$g_{\mathrm{O-H}}(r_{M1})$	1.433 (0.144)	1.426 (0.144)	1.405 (0.144)	1.378 (0.144)	1.358 (0.144)
$g_{\mathrm{O-H}}(r_{m1})$	0.195 (0.196)	0.196 (0.196)	0.199 (0.196)	0.203 (0.194)	0.207 (0.194)
$n_{\mathrm{O-H}}(r_{m1})$	0.65 (0.196)	0.65 (0.196)	0.65 (0.196)	0.65 (0.194)	0.66 (0.194)
$g_{\mathrm{Li^+-O}}(r_{M1})$	7.475 (0.188)	7.450 (0.188)	7.377 (0.188)	7.280 (0.188)	7.190 (0.188)
$g_{\mathrm{Li^+-O}}(r_{m1})$	0.145 (0.264)	0.145 (0.264)	0.147 (0.264)	0.150 (0.264)	0.153 (0.264)
$n_{\mathrm{Li^+-O}}(r_{m1})$	2.41 (0.264)	2.43 (0.264)	2.45 (0.264)	2.49 (0.264)	2.53 (0.264)
$g_{\mathrm{Li^+-H}}(r_{M1})$	1.562 (0.274)	1.560 (0.274)	1.555 (0.274)	1.549 (0.274)	1.545 (0.274)
$g_{\mathrm{Li^+-H}}(r_{m1})$	0.793 (0.348)	0.793 (0.348)	0.796 (0.348)	0.799 (0.348)	0.801 (0.348)
$n_{\mathrm{Li^+-H}}(r_{m1})$	7.80 (0.348)	7.85 (0.348)	7.99 (0.348)	8.18 (0.348)	8.38 (0.348)
$g_{\mathrm{Cl^--O}}(r_{M1})$	2.749 (0.344)	2.755 (0.344)	2.771 (0.344)	2.791 (0.344)	2.810 (0.342)
$g_{\mathrm{Cl^--O}}(r_{m1})$	0.781 (0.462)	0.779 (0.462)	0.774 (0.462)	0.767 (0.460)	0.761 (0.460)
$n_{\mathrm{Cl^--O}}(r_{m1})$	10.85 (0.462)	10.92 (0.462)	11.10 (0.462)	11.22 (0.460)	11.45 (0.460)
$g_{\mathrm{Cl^--H}}(r_{M1})$	2.254 (0.198)	2.247 (0.198)	2.227 (0.198)	2.201 (0.198)	2.180 (0.198)
$g_{\mathrm{Cl^--H}}(r_{m1})$	0.410 (0.262)	0.412 (0.262)	0.418 (0.262)	0.426 (0.262)	0.435 (0.262)
$n_{\mathrm{Cl^--H}}(r_{m1})$	2.54 (0.262)	2.55 (0.262)	2.59 (0.262)	2.65 (0.262)	2.71 (0.262)
$g_{\mathrm{Li^+-Cl^-}}(r_{M1})$	21.732 (0.220)	21.442 (0.220)	20.718 (0.220)	19.848 (0.220)	18.977 (0.220)
$g_{\mathrm{Li^+-Cl^-}}(r_{m1})$	0.701 (0.338)	0.702 (0.338)	0.705 (0.338)	0.711 (0.336)	0.717 (0.336)
$n_{\mathrm{Li^+-Cl^-}}(r_{m1})$	1.24 (0.338)	1.23 (0.338)	1.22 (0.338)	1.20 (0.336)	1.19 (0.336)
$g_{\mathrm{Li^+-Cl^-}}(r_{M2})$	1.398 (0.470–0.480)[b]	1.398 (0.470–0.476)[b]	1.399 (0.466–0.474)[b]	1.405 (0.464–0.472)[b]	1.412 (0.462–0.468)[b]
$g_{\mathrm{Li^+-Cl^-}}(r_{m2})$	0.831 (0.620)	0.830 (0.620)	0.825 (0.618)	0.819 (0.616)	0.814 (0.614)
$n_{\mathrm{Li^+-Cl^-}}^{(\mathrm{II})}(r_{m2})$	1.64 (0.620)	1.66 (0.620)	1.67 (0.618)	1.70 (0.616)	1.72 (0.614)
$g_{\mathrm{Li^+-Li^+}}(r_{M1})$	1.166 (0.368)	1.148 (0.368)	1.108 (0.368)	1.066 (0.368)	1.025 (0.368)
$g_{\mathrm{Li^+-Li^+}}(r_{m1})$	0.994 (0.402)	0.980 (0.402)	0.946 (0.402)	0.909 (0.402)	0.873 (0.402)
$n_{\mathrm{Li^+-Li^+}}^{(\mathrm{I})}(r_{m1})$	0.28 (0.402)	0.27 (0.402)	0.27 (0.402)	0.26 (0.402)	0.26 (0.402)
$g_{\mathrm{Li^+-Li^+}}(r_{M2})$	1.066 (0.430)	1.052 (0.430)	1.020 (0.432)	0.985 (0.432)	0.954 (0.434)
$g_{\mathrm{Li^+-Li^+}}(r_{m2})$	0.919 (0.478)	0.917 (0.476)	0.914 (0.474)	0.910 (0.472)	0.906 (0.470)
$n_{\mathrm{Li^+-Li^+}}^{(\mathrm{II})}(r_{m2})$	0.33 (0.478)	0.32 (0.476)	0.31 (0.474)	0.31 (0.472)	0.29 (0.470)
$g_{\mathrm{Cl^--Cl^-}}(r_{M1})$	3.033 (0.364)	3.022 (0.364)	3.015 (0.362)	3.032 (0.360)	3.053 (0.358)
$g_{\mathrm{Cl^--Cl^-}}(r_{m1})$	0.434 (0.496)	0.432 (0.496)	0.424 (0.496)	0.414 (0.494)	0.405 (0.494)
$n_{\mathrm{Cl^--Cl^-}}(r_{m1})$	0.95 (0.496)	0.95 (0.496)	0.95 (0.496)	0.95 (0.494)	0.96 (0.494)

[a] r_M, position of the peak maximum; $g_{\alpha\beta}(r_M)$, peak height; r_m, position of the minimum; $g_{\alpha\beta}(r_m)$, function value in this point; $n_{\alpha\beta}(r_m)$, number of particles of kind β at a distance r_m from a particle of kind α (all the distances are given in nm). [b] Ranges of shoulders and diffuse peaks and the corresponding values of functions.

slightly shifts down. In the entire pressure range, the second minimum noticeably shifts toward shorter r, but the function $n_{\mathrm{O-O}}^{(\mathrm{I+II})}(r_{m2})$ remains virtually unchanged owing to the growth of the solution density.

In the LiCl : 8.05H_2O solution (Table 2), compression affects the pair correlation function $g_{\mathrm{O-O}}(r)$ similarly. However, in this case the function has the first minimum at a distance of 0.448 nm (at 100 bar), with the lacking second minimum. As the pressure is increased, the first minimum appreciably shifts toward shorter distances; as a result, $n_{\mathrm{O-O}}^{(\mathrm{I})}(r_{m1})$ decreases by 3.9%.

In the LiCl : 3.15H_2O solution, the pressure has virtually no effect on the $g_{\mathrm{O-O}}(r)$ function, and $n_{\mathrm{O-O}}^{(\mathrm{I})}(r_{m1})$ increases by 3.6% owing to the growth of the solution density (Table 3).

Table 2. Characteristic values of some pair correlation functions $g_{\alpha\beta}(r)$ and functions $n_{\alpha\beta}(r)$ for the LiCl : $8.05H_2O$ system under conditions of isothermal compression (T 523 K, P 100–1500 bar)

Parameter[a]	100 bar	200 bar	500 bar	1000 bar	1500 bar
$g_{O-O}(r_{M1})$	2.396 (0.290)	2.407 (0.290)	2.429 (0.290)	2.458 (0.290)	2.490 (0.290)
$g_{O-O}(r_{m1})$	0.878 (0.448)	0.876 (0.446)	0.872 (0.440)	0.867 (0.436)	0.861 (0.432)
$n^{(I)}_{O-O}(r_{m1})$	9.17 (0.448)	9.12 (0.446)	8.91 (0.440)	8.85 (0.436)	8.81 (0.432)
$g_{O-H}(r_{M1})$	1.287 (0.144)	1.279 (0.144)	1.264 (0.144)	1.245 (0.144)	1.224 (0.144)
$g_{O-H}(r_{m1})$	0.199 (0.194)	0.201 (0.194)	0.203 (0.194)	0.207 (0.194)	0.211 (0.194)
$n_{O-H}(r_{m1})$	0.57 (0.194)	0.57 (0.194)	0.58 (0.194)	0.58 (0.194)	0.59 (0.194)
$g_{Li^+-O}(r_{M1})$	7.103 (0.188)	7.076 (0.188)	7.023 (0.188)	6.957 (0.188)	6.883 (0.188)
$g_{Li^+-O}(r_{m1})$	0.141 (0.264)	0.142 (0.264)	0.144 (0.264)	0.146 (0.262)	0.148 (0.262)
$n_{Li^+-O}(r_{m1})$	2.22 (0.264)	2.23 (0.264)	2.25 (0.264)	2.27 (0.262)	2.30 (0.262)
$g_{Li^+-H}(r_{M1})$	1.550 (0.274)	1.548 (0.274)	1.546 (0.274)	1.543 (0.274)	1.541 (0.274)
$g_{Li^+-H}(r_{m1})$	0.812 (0.348)	0.813 (0.348)	0.815 (0.348)	0.817 (0.348)	0.819 (0.348)
$n_{Li^+-H}(r_{m1})$	7.54 (0.348)	7.60 (0.348)	7.71 (0.348)	7.85 (0.348)	8.01 (0.348)
$g_{Cl^--O}(r_{M1})$	2.800 (0.344)	2.805 (0.344)	2.815 (0.344)	2.828 (0.342)	2.845 (0.342)
$g_{Cl^--O}(r_{m1})$	0.762 (0.462)	0.760 (0.462)	0.756 (0.462)	0.751 (0.460)	0.745 (0.460)
$n_{Cl^--O}(r_{m1})$	10.52 (0.462)	10.58 (0.462)	10.70 (0.462)	10.75 (0.460)	10.92 (0.460)
$g_{Cl^--H}(r_{M1})$	2.115 (0.198)	2.109 (0.198)	2.096 (0.198)	2.080 (0.198)	2.063 (0.198)
$g_{Cl^--H}(r_{m1})$	0.422 (0.260)	0.425 (0.260)	0.430 (0.260)	0.436 (0.260)	0.444 (0.260)
$n_{Cl^--H}(r_{m1})$	2.33 (0.260)	2.35 (0.260)	2.38 (0.260)	2.42 (0.260)	2.46 (0.260)
$g_{Li^+-Cl^-}(r_{M1})$	14.864 (0.220)	14.685 (0.220)	14.356 (0.220)	13.973 (0.220)	13.547 (0.220)
$g_{Li^+-Cl^-}(r_{m1})$	0.563 (0.336)	0.565 (0.336)	0.569 (0.336)	0.575 (0.336)	0.582 (0.336)
$n^{(I)}_{Li^+-Cl^-}(r_{m1})$	1.56 (0.336)	1.56 (0.336)	1.55 (0.336)	1.54 (0.336)	1.54 (0.336)
$g_{Li^+-Cl^-}(r_{M2})$	1.085–1.226 (0.430–0.470)[b]	1.089–1.229 (0.430–0.470)[b]	1.099–1.234 (0.430–0.470)[b]	1.110–1.241 (0.430–0.470)[b]	1.123–1.249 (0.430–0.470)[b]
$g_{Li^+-Cl^-}(r_{M2'})$	1.249 (0.496)	1.250 (0.496)	1.252 (0.496)	1.526 (0.494)	1.262 (0.492)
$g_{Li^+-Cl^-}(r_{m2})$	0.813 (0.618)	0.811 (0.618)	0.809 (0.618)	0.805 (0.616)	0.802 (0.614)
$n^{(II)}_{Li^+-Cl^-}(r_{m2})$	2.64 (0.618)	2.66 (0.618)	2.70 (0.618)	2.73 (0.616)	2.76 (0.614)
$g_{Li^+-Li^+}(r_{M1})$	1.160 (0.368)	1.152 (0.368)	1.137 (0.368)	1.123 (0.368)	1.108 (0.368)
$g_{Li^+-Li^+}(r_{m1})$	0.994 (0.404)	0.987 (0.404)	0.974 (0.404)	0.959 (0.404)	0.945 (0.404)
$n^{(I)}_{Li^+-Li^+}(r_{m1})$	0.51 (0.404)	0.51 (0.404)	0.51 (0.404)	0.51 (0.404)	0.52 (0.404)
$g_{Li^+-Li^+}(r_{M2})$	1.066 (0.434)	1.089 (0.434)	1.047 (0.434)	1.034 (0.436)	1.021 (0.436)
$g_{Li^+-Li^+}(r_{m2})$	0.958 (0.480)	0.959 (0.478)	0.961 (0.478)	0.963 (0.476)	0.966 (0.474)
$n^{(II)}_{Li^+-Li^+}(r_{m2})$	0.61 (0.480)	0.60 (0.478)	0.59 (0.478)	0.58 (0.476)	0.57 (0.474)
$g_{Cl^--Cl^-}(r_{M1})$	2.843 (0.360)	2.853 (0.360)	2.878 (0.360)	2.920 (0.358)	2.975 (0.356)
$g_{Cl^--Cl^-}(r_{m1})$	0.446 (0.496)	0.444 (0.496)	0.438 (0.496)	0.431 (0.494)	0.423 (0.494)
$n_{Cl^--Cl^-}(r_{m1})$	1.59 (0.496)	1.60 (0.496)	1.62 (0.496)	1.64 (0.494)	1.66 (0.494)

[a] For designations, see note to Table 1. [b] See note to Table 1.

O–H. Isothermal compression causes the intensity of the first peak of the $g_{O-H}(r)$ function to decrease for all the solutions, with the O–H distance and the position of the first minimum remaining unchanged. The second peak slightly shifts toward shorter distances and very slightly grows in intensity. It should be noted that the effect of pressure on the $g_{O-H}(r)$ function weakens in going to more concentrated solutions. Calculations showed that, in all the three systems, the number of O–H bonds does not change noticeably owing to increasing solution density (Tables 1–3).

H–H. Irrespective of the solution concentration, the first peak in the pair correlation function $g_{H-H}(r)$ slightly grows in height with increasing pressure at high temperature, whereas the height of the second peak remains virtually unchanged.

Table 3. Characteristic values of some pair correlation functions $g_{\alpha\beta}(r)$ and functions $n_{\alpha\beta}(r)$ for the LiCl : $3.15H_2O$ system under conditions of isothermal compression (T 523 K, P 100–1500 bar)

Parameter[a]	100 bar	200 bar	500 bar	1000 bar	1500 bar
$g_{\mathrm{O-O}}(r_{M1})$	2.663 (0.288)	2.671 (0.288)	2.693 (0.288)	2.722 (0.286)	2.744 (0.286)
$g_{\mathrm{O-O}}(r_{m1})$	0.823 (0.428)	0.821 (0.428)	0.818 (0.428)	0.814 (0.428)	0.811 (0.428)
$n^{(\mathrm{I})}_{\mathrm{O-O}}(r_{m1})$	7.12 (0.428)	7.15 (0.428)	7.23 (0.428)	7.32 (0.428)	7.38 (0.428)
$g_{\mathrm{O-H}}(r_{M1})$	0.969 (0.146)	0.966 (0.146)	0.957 (0.146)	0.947 (0.146)	0.940 (0.146)
$g_{\mathrm{O-H}}(r_{m1})$	0.209 (0.190)	0.210 (0.190)	0.212 (0.190)	0.215 (0.190)	0.217 (0.190)
$n_{\mathrm{O-H}}(r_{m1})$	0.39 (0.190)	0.39 (0.190)	0.39 (0.190)	0.40 (0.190)	0.40 (0.190)
$g_{\mathrm{Li^+-O}}(r_{M1})$	6.346 (0.188)	6.334 (0.188)	6.300 (0.188)	6.258 (0.188)	6.228 (0.188)
$g_{\mathrm{Li^+-O}}(r_{m1})$	0.135 (0.262)	0.136 (0.262)	0.137 (0.262)	0.139 (0.262)	0.140 (0.262)
$n_{\mathrm{Li^+-O}}(r_{m1})$	1.72 (0.262)	1.73 (0.262)	1.74 (0.262)	1.75 (0.262)	1.76 (0.262)
$g_{\mathrm{Li^+-H}}(r_{M1})$	1.524 (0.274)	1.524 (0.274)	1.523 (0.274)	1.523 (0.274)	1.523 (0.274)
$g_{\mathrm{Li^+-H}}(r_{m1})$	0.842 (0.348)	0.842 (0.348)	0.843 (0.348)	0.844 (0.348)	0.845 (0.348)
$n_{\mathrm{Li^+-H}}(r_{m1})$	6.54 (0.348)	6.56 (0.348)	6.63 (0.348)	6.71 (0.348)	6.76 (0.348)
$g_{\mathrm{Cl^--O}}(r_{M1})$	2.849 (0.342)	2.851 (0.342)	2.855 (0.342)	2.859 (0.342)	2.861 (0.342)
$g_{\mathrm{Cl^--O}}(r_{m1})$	0.718 (0.462)	0.717 (0.462)	0.714 (0.460)	0.711 (0.460)	0.709 (0.460)
$n_{\mathrm{Cl^--O}}(r_{m1})$	9.01 (0.462)	9.01 (0.462)	9.01 (0.460)	9.08 (0.460)	9.12 (0.460)
$g_{\mathrm{Cl^--H}}(r_{M1})$	1.828 (0.198)	1.827 (0.198)	1.821 (0.198)	1.814 (0.198)	1.809 (0.198)
$g_{\mathrm{Cl^--H}}(r_{m1})$	0.449 (0.260)	0.450 (0.260)	0.454 (0.260)	0.458 (0.260)	0.461 (0.260)
$n_{\mathrm{Cl^--H}}(r_{m1})$	1.87 (0.260)	1.88 (0.260)	1.90 (0.260)	1.92 (0.260)	1.94 (0.260)
$g_{\mathrm{Li^+-Cl^-}}(r_{M1})$	9.654 (0.220)	9.618 (0.220)	9.512 (0.220)	9.398 (0.220)	9.320 (0.220)
$g_{\mathrm{Li^+-Cl^-}}(r_{m1})$	0.467 (0.336)	0.469 (0.336)	0.472 (0.336)	0.476 (0.336)	0.479 (0.336)
$n^{(\mathrm{I})}_{\mathrm{Li^+-Cl^-}}(r_{m1})$	2.37 (0.336)	2.37 (0.336)	2.37 (0.336)	2.38 (0.336)	2.39 (0.336)
$g_{\mathrm{Li^+-Cl^-}}(r_{M2})$	0.930–1.115 (0.430–0.470)[b]	0.932–1.117 (0.430–0.470)[b]	0.938–1.120 (0.430–0.470)[b]	0.945–1.125 (0.430–0.470)[b]	0.949–1.128 (0.430–0.470)[b]
$g_{\mathrm{Li^+-Cl^-}}(r_{M2'})$	1.199 (0.508)	1.200 (0.508)	1.201 (0.508)	1.203 (0.508)	1.205 (0.508)
$g_{\mathrm{Li^+-Cl^-}}(r_{m2})$	0.832 (0.630)	0.832 (0.630)	0.830 (0.628)	0.828 (0.628)	0.826 (0.628)
$n^{(\mathrm{II})}_{\mathrm{Li^+-Cl^-}}(r_{m2})$	5.98 (0.630)	6.00 (0.630)	6.01 (0.628)	6.08 (0.628)	6.13 (0.628)
$g_{\mathrm{Li^+-Li^+}}(r_{M1})$	1.392 (0.366)	1.391 (0.366)	1.390 (0.366)	1.389 (0.366)	1.388 (0.366)
$g_{\mathrm{Li^+-Li^+}}(r_{m1})$	1.188 (0.410)	1.187 (0.410)	1.183 (0.410)	1.179 (0.410)	1.177 (0.410)
$n^{(\mathrm{I})}_{\mathrm{Li^+-Li^+}}(r_{m1})$	1.48 (0.410)	1.49 (0.410)	1.50 (0.410)	1.52 (0.410)	1.54 (0.410)
$g_{\mathrm{Li^+-Li^+}}(r_{M2})$	1.217 (0.430)	1.215 (0.430)	1.212 (0.430)	1.208 (0.430)	1.206 (0.430)
$g_{\mathrm{Li^+-Li^+}}(r_{m2})$	0.976 (0.498)	0.977 (0.498)	0.980 (0.498)	0.983 (0.498)	0.985 (0.498)
$n^{(\mathrm{II})}_{\mathrm{Li^+-Li^+}}(r_{m2})$	1.78 (0.498)	1.78 (0.498)	1.80 (0.498)	1.82 (0.498)	1.83 (0.498)
$g_{\mathrm{Cl^--Cl^-}}(r_{M1})$	2.880 (0.356)	2.888 (0.354)	2.916 (0.354)	2.950 (0.354)	2.977 (0.352)
$g_{\mathrm{Cl^--Cl^-}}(r_{m1})$	0.471 (0.498)	0.470 (0.496)	0.466 (0.496)	0.463 (0.496)	0.460 (0.496)
$n_{\mathrm{Cl^--Cl^-}}(r_{m1})$	3.58 (0.498)	3.58 (0.496)	3.61 (0.496)	3.65 (0.496)	3.68 (0.496)

[a] For designations, see note to Table 1. [b] See note to Table 1.

Our results show that, on the whole, compression at a high temperature affects the structure of the bulk solvent in the LiCl–H_2O system similarly to compression at the standard temperature [19]. The changes in the solvent structure are similar to those observed in pure water upon compression [20].

ION–WATER (I–W) CORRELATIONS

Li^+–O. The pair correlation functions $g_{\mathrm{Li^+-O}}(r)$ for the system LiCl : $14.90H_2O$, plotted in Fig. 2, and the characteristic values of these functions, listed in Table 1, show that the isothermal compression is accompanied by a slight decrease in the height of the main peak in this function. At the same time, the pressure growth does not affect the distance between the lithium ion and the water molecules from its first coordination sphere; the position of the first minimum of the function $g_{\mathrm{Li^+-O}}(r)$ is not affected either. Despite such trends, the number of water molecules in the first coordination sphere of the Li^+ ion [$n_{\mathrm{Li^+-O}}(r_{m1})$] in-

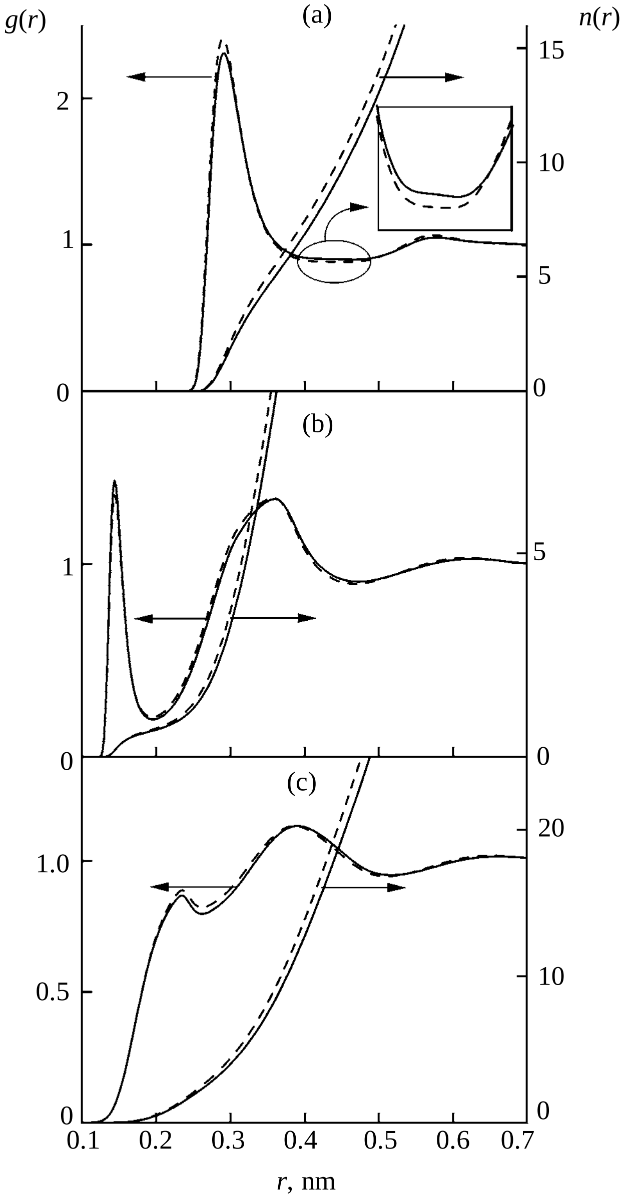

Fig. 1. Pair correlation functions (a) $g_{\mathrm{O-O}}(r)$, (b) $g_{\mathrm{O-H}}(r)$, and (c) $g_{\mathrm{H-H}}(r)$, and functions (a) $n_{\mathrm{O-O}}(r)$, (b) $n_{\mathrm{O-H}}(r)$, and (c) $n_{\mathrm{H-H}}(r)$ for the LiCl : 14.90H_2O solution at 523 K and pressures of (solid line) 100 and (dashed line) 1500 bar.

creases by 5%, which is due to the growth of the solution density.

In more concentrated solutions, under similar conditions, the trends in variation of $g_{\mathrm{Li^+-O}}(r)$ are similar but the effect of compression weakens. In the LiCl : 8.05H_2O solution, $n_{\mathrm{Li^+-O}}(r_{m1})$ increases by 3.6%, and in the LiCl : 3.15H_2O solution, by only 2.3% (Table 3).

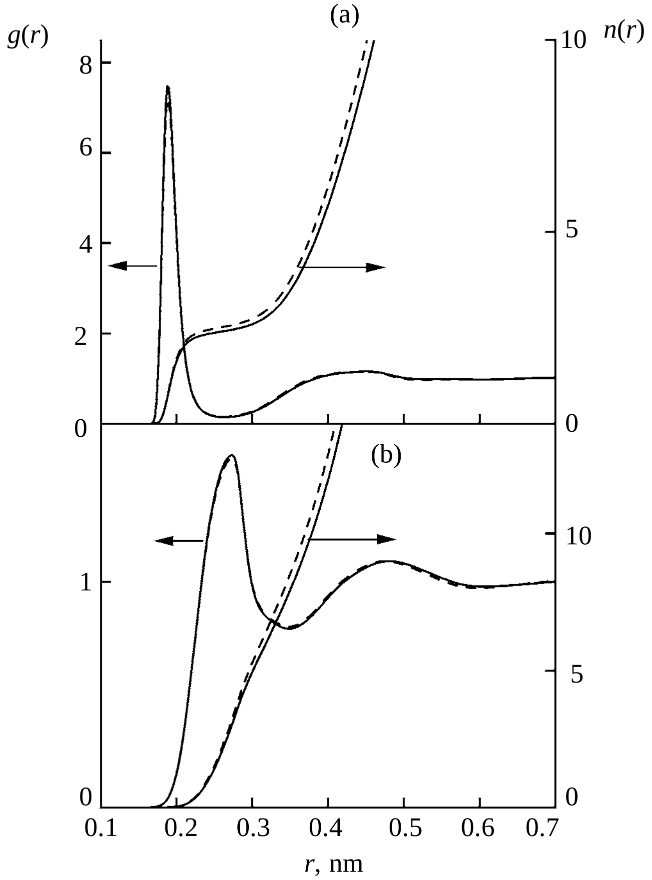

Fig. 2. Pair correlation functions (a) $g_{\mathrm{Li^+-O}}(r)$ and (b) $g_{\mathrm{Li^+-H}}(r)$, and functions (a) $n_{\mathrm{Li^+-O}}(r)$ and (b) $n_{\mathrm{Li^+-H}}(r)$ for the LiCl : 14.90H_2O solution at 523 K and pressures of (solid line) 100 and (dashed line) 1500 bar.

$\mathrm{Li^+}$–H. Figure 2 and Table 1 show that compression of the LiCl : 14.90H_2O solution has virtually no effect on the height of the main peak of the $g_{\mathrm{Li^+-H}}(r)$ function. As in the pair correlation function $g_{\mathrm{Li^+-O}}(r)$, the positions of the maximum and first minimum remain unchanged. In more concentrated solutions, the effect of pressure also becomes less noticeable. For example, in the systems LiCl : 14.90H_2O, LiCl : 8.05H_2O, and LiCl : 3.15H_2O, $n_{\mathrm{Li^+-O}}(r_{m1})$ increased by 7.4 (Table 1), 6.2 (Table 2) and 3.4% (Table 3), respectively.

$\mathrm{Cl^-}$–O. Figure 3 and Table 1 show that isothermal compression of the LiCl : 14.90H_2O system causes the main peak of the $g_{\mathrm{Cl^--O}}(r)$ function to slightly increase, with the positions of its maximum and first minimum slightly shifting toward shorter distances. Calculations show that $n_{\mathrm{Cl^--O}}(r_{m1})$ increases by 5.5% in the pressure range from 100 to 1500 bar. In more concentrated solutions, the effect of pressure on the

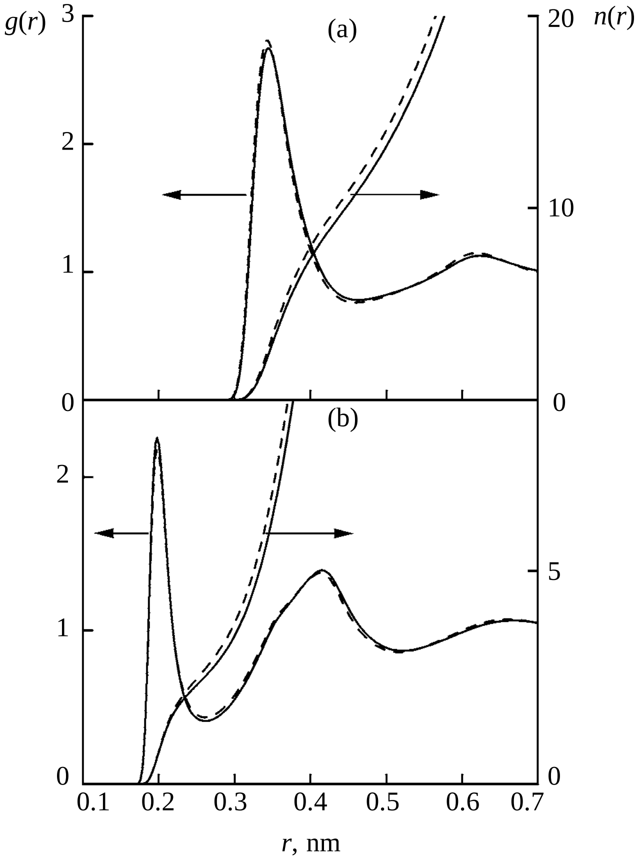

Fig. 3. Pair correlation functions (a) $g_{Cl^-–O}(r)$ and (b) $g_{Cl^-–H}(r)$, and functions (a) $n_{Cl^-–O}(r$ and (b) $n_{Cl^-–H}(r)$ for the LiCl : 14.90H_2O solution at 523 K and pressures of (solid line) 100 and (dashed line) 1500 bar.

coordinative power of the chloride ion weakens. For example, in the LiCl : 8.05H_2O system, $n_{Cl^-–O}(r_{m1})$ increases by 3.8% (Table 2), and in the LiCl : 3.15H_2O system it remains constant in the range 100–500 bar and increases by 1.2% only when the pressure is raised from 500 to 1500 bar (Table 3).

Cl^-–H. As in the case of the $g_{O–H}(r)$ function, in all the three systems the main peak of the $g_{Cl^-–H}(r)$ function slightly decreases with increasing pressure (Fig. 3, Tables 1–3), with the positions of its maximum and first minimum remaining unchanged. Nevertheless, the number of hydrogen bonds slightly grows owing to an increase in the solution density; the effect of pressure on $n_{Cl^-–H}(r_{m1})$ is stronger in less concentrated solutions. For example, in the LiCl : 14.90H_2O, LiCl : 8.05H_2O, and LiCl : 3.15H_2O solutions, $n_{Cl^-–H}(r_{m1})$ increased by 6.7 (Table 1), 5.6 (Table 2), and 3.7% (Table 3).

Similar results were obtained in a neutron diffraction study of a 10 M LiCl solution [5]. It was shown that compression to 1 kbar had virtually no effect on the Cl^-–O and Cl^-–D distances and the coordination number of the chloride ion. This behavior was attributed to the fact that the dynamic behavior of systems containing the Li^+ ion is virtually insensitive to pressure elevation up to 4 kbar.

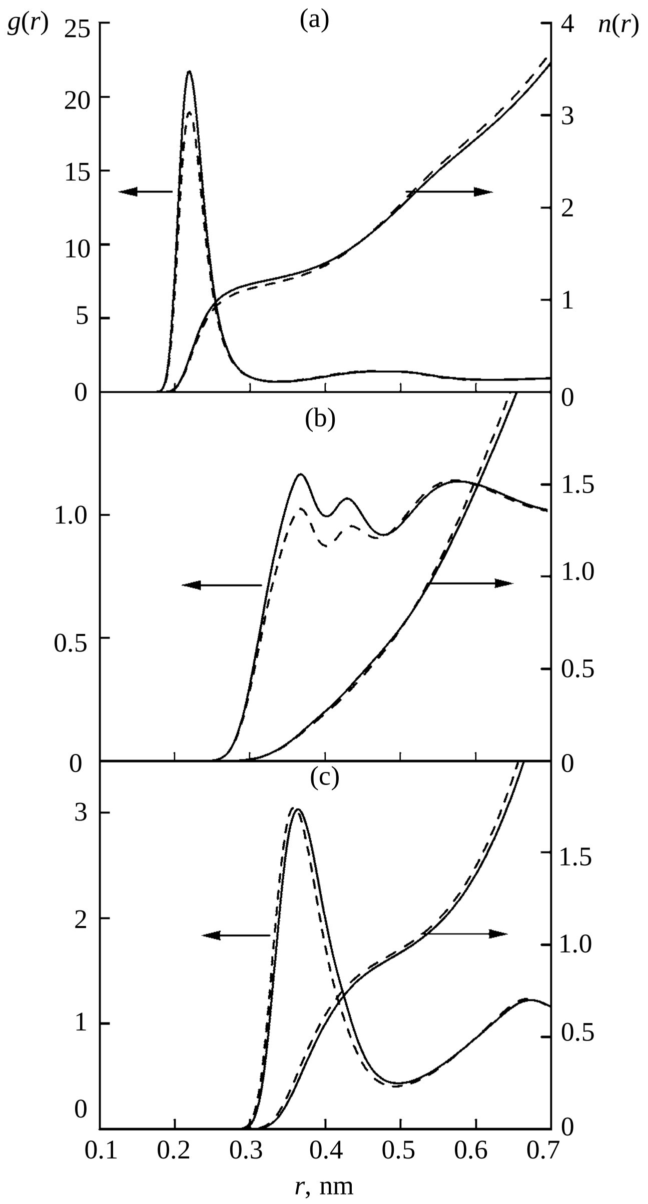

Fig. 4. Pair correlation functions (a) $g_{Li^+–Cl^-}(r)$, (b) $g_{Li^+–Li^+}(r)$, and (c) $g_{Cl^-–Cl^-}(r)$, and functions (a) $n_{Li^+–Cl^-}(r)$, (b) $n_{Li^+–Li^+}(r)$, and (c) $n_{Cl^-–Cl^-}(r)$ for the LiCl : 14.90H_2O solution at 523 K and pressures of (solid line) 100 and (dashed line) 1500 bar.

Comparison of the relative changes in the numbers of water molecules in the first coordination spheres of the cation and anion $[\Delta n_{\mathrm{Cl^-{-}H}}(r_{m1})$ and $\Delta n_{\mathrm{Li^+{-}H}}(r_{m1})]$ shows that, in the LiCl : 14.90H_2O and LiCl : 8.05H_2O solutions, isothermal compression affects the coordinative power of the ions similarly, whereas in the LiCl : 3.15H_2O system the effect of pressure on the coordinative power of the Li^+ ion is stronger $[\Delta n_{\mathrm{Li^+{-}H}}(r_{m1}) > \Delta n_{\mathrm{Cl^-{-}H}}(r_{m1})]$.

Note that the trends in variation of the parameters of hydration of the Li^+ and Cl^- ions under the conditions of isothermal compression are nicely consistent on the qualitative level with the results of numerous experimental and theoretical studies (see, e.g., [6, 21, 22]).

ION–ION (I–I) CORRELATIONS

The results given in Tables 1–3 for aqueous LiCl solutions show that, irrespective of the solution concentration, the compression at high temperatures causes the first peak of the $g_{\mathrm{Li^+{-}Cl^-}}(r)$ function to decrease, with its position remaining unchanged. The first minimum slightly shifts toward shorter distances only in the LiCl : 14.90H_2O solution (Fig. 4, Table 1). Calculations show that, in less concentrated solutions, the number of contact ion pairs $[n^{\mathrm{(I)}}_{\mathrm{Li^+{-}Cl^-}}(r_{m1})]$ slightly decreases: by 4% in the LiCl : 14.90H_2O solution (Table 1) and by only 1.3% in the LiCl : 8.05H_2O solution (Table 2). In the LiCl : 3.15H_2O solution, in the pressure range 100–500 bar, $n^{\mathrm{(I)}}_{\mathrm{Li^+{-}Cl^-}}(r_{m1})$ does not change, and only further compression (and hence increase in the solution density) causes this quantity to slightly (by 0.8%) grow (Table 3).

We have shown previously [16] that, in LiCl solutions of similar concentrations at 523 K and pressure close to the standard value, the second peak of the pair correlation function $g_{\mathrm{Li^+{-}Cl^-}}(r)$ is diffuse. With further compression, its shape and intensity remain virtually unchanged, and only due to an increase in the solution density the number of hydration-separated ion pairs $[n^{\mathrm{(II)}}_{\mathrm{Li^+{-}Cl^-}}(r_{m2})]$ increases by almost 5%.

In more concentrated solutions, compression also has virtually no effect on $g_{\mathrm{Li^+{-}Cl^-}}(r)$ in the vicinity of the second peak. The number of hydration-separated ion pairs increases owing to the growth of the solution density. For example, in the LiCl : 8.05H_2O solution, $n^{\mathrm{(II)}}_{\mathrm{Li^+{-}Cl^-}}(r_{m2})$ increased by 4.5%, and in the LiCl : 3.15H_2O solution, by 2.5%.

Comparison of the relative changes in $n^{\mathrm{(I)}}_{\mathrm{Li^+{-}Cl^-}}(r_{m1})$ and $n^{\mathrm{(II)}}_{\mathrm{Li^+{-}Cl^-}}(r_{m2})$ shows that the isothermal compression affects the number of hydration-separated ion pairs to a greater extent than the number of contact ion pairs $[n^{\mathrm{(II)}}_{\mathrm{Li^+{-}Cl^-}}(r_{m2}) > n^{\mathrm{(I)}}_{\mathrm{Li^+{-}Cl^-}}(r_{m1})]$.

Figure 4 and Tables 1–3 show that, in all the systems under consideration, isothermal compression causes a certain decrease in the number of Li^+–H 2O–Li^+ associates, with the distances between the ions remaining the same. At the same time, with increasing pressure, the distance between the chloride ions in the Cl^-–Cl^- contact ion pair slightly decreases, with the number of such associates remaining virtually the same. It should be noted, however, that molecular-dynamics and Monte Carlo simulation of aqueous NaCl solution led Hummer *et al.* to a conclusion that the theory of integral equations tends to overestimate the probability of pairing of similarly charged ions [23]. Hummer et al. believe that this drawback is inherent in the method. Thus, the results reported here for the functions $g_{\mathrm{Li^+{-}Li^+}}(r)$ and $g_{\mathrm{Cl^-{-}Cl^-}}(r)$ are only illustrative; they demonstrate the possibility of obtaining the whole set of pair correlation functions by the method of integral equations.

Thus, isothermal compression only weakly affects the structure of the bulk solvent in aqueous LiCl solutions; the only effect is that the density of less concentrated solutions slightly increases. Irrespective of the solution concentration, the tetrahedral ordering of solvent molecules is absent in the entire pressure range, and the number of O–H bonds remains virtually unchanged. With increasing pressure, the coordinative power of both ions in all the solutions slightly grows; the content of hydration-separated ion pairs somewhat increases, and the content of contact ion pairs slightly decreases. These results show that the effect exerted by isothermal compression on structure formation in aqueous LiCl solutions is similar to the effect of compression at the standard temperature [19], but in the former case the structural changes are more appreciable.

ACKNOWLEDGMENTS

The study was financially supported by the Russian Foundation for Basic Research (project no. 01-03-32 278).

REFERENCES

1. Oparin, R.D., Fedotova, M.V., and Trostin, V.N., *Zh. Obshch. Khim.*, 1998, vol. 68, no. 10, p. 1625.
2. Oparin, R.D., Fedotova, M.V., Vinogradov, E.V., and Trostin, V.N., Available from VINITI, Moscow, 1999, no. 414-V99.
3. Oparin, R.D., Fedotova, M.V., and Trostin, V.N., *Izv. Ross. Akad. Nauk, Ser. Khim.*, 1999, no. 10, p. 1881.
4. Oparin, R.D., Fedotova, M.V., Vinogradov, E.V., and Trostin, V.N., Available from VINITI, Moscow, 2000, no. 16-V00.

5. Neilson, G.W., *Chem. Phys. Lett.*, 1979, vol. 68, no. 2/3, p. 247.
6. Frank, E.U., *Chemistry and Geochemistry of Solution at High Temperatures and Pressures. Physical Chemistry of the Earth,* Rickard, D.T. and Wickman, F.W., Eds., Oxford: Pergamon, 1981, vol. 13/14, p. 65.
7. Nakahara, M. and Osugi, J., *Rev. Phys. Chem. Jpn.*, 1975, vol. 45, no. 2, p. 69; 1980, vol. 50, no. 2, p. 66.
8. Jancso, G., Heinzinger, K., and Bopp, P., *Z. Naturforsch. A*, 1985, vol. 40, no. 12, p. 1235.
9. Jancso, G., Heinzinger, K., and Radnai, T., *Chem. Phys. Lett.*, 1984, vol. 110, no. 1, p. 196.
10. Errington, J.R., *Fluid Phase Equil.*, 1998, vols. 150–151, p. 33.
11. Berendsen, H.J.C., Postma, J.P.M., Van Gunsteren, W.F., and Hermans, J., Abstracts of Papers, *Jerusalem Symp. on Quantum Chemistry and Biochemistry,* Pullman, B., Ed., Dordrecht: Reidel, 1981, p. 331.
12. Pettitt, B.M. and Rossky, P.J., *J. Chem. Phys.*, 1982, vol. 77, no. 3, p. 1451.
13. Pettitt, B.M. and Rossky, P.J., *J. Chem. Phys.*, 1986, vol. 84, no. 10, p. 5836.
14. Chandler, D. and Andersen, H.C., *J. Chem. Phys.*, 1972, vol. 57, no. 5, p. 1930.
15. Kalyuzhnyi, Yu.V., Fedotova, M.V., Golovko, M.F., and Trostin, V.N., *Preprint of the Inst. of Physics of Condensed Systems, National Acad. Sci. of the Ukraine,* Lviv, 1994, no. IFKS-93-27R.
16. Oparin, R.D., Fedotova, M.V., and Trostin, V.N., Abstracts of Papers, *Mezhdunarodnaya konferentsiya “Zhidkofaznye sistemy i nelineinye protsessy v khimii i khimicheskoi tekhnologii”* (Int. Conf. “Liquid-Phase Systems and Nonlinear Processes in Chemistry and Chemical Technology”), Ivanovo, 1999, p. 41.
17. Kalyuzhnyi, Yu.V., Fedotova, M.V., Golovko, M.F., and Trostin, V.N., *Preprint of the Inst. of Theoretical Physics, Acad. Sci. of Ukr. SSR*, Kiev, 1991, no. 91-19R.
18. Narten, A.H., *Report of the Oak Ridge National Laboratory,* 1970, no. 4578.
19. Oparin, R.D., Fedotova, M.V., and Trostin, V.N., Abstracts of Papers, *II Mezhdunarodnaya nauchno-tekhnicheskaya konferentsiya* (II Int. Scientific and Technical Conf.), Ivanovo, 1999, p. 18.
20. Pettitt, B.M. and Calef, D.F., *J. Phys. Chem.*, 1987, vol. 91, no. 6, p. 1541.
21. Neilson, G.W., *Chem. Phys. Lett.*, 1979, vol. 68, no. 2/3, p. 247.
22. Haman, S.D., *Chemistry and Geochemistry of Solution at High Temperatures and Pressures. Physical Chemistry of the Earth,* Rickard, D.T. and Wickman, F.W., Eds., Oxford: Pergamon, 1981, vol. 13/14, p. 89.
23. Hummer, G., Soumpasis, D.M., and Neumann, M., *Mol. Phys.*, 1993, vol. 81, no. 5, p. 1155.